Journal of Solid State Chemistry **149,** 143–148 (2000)
Article ID jssc.1999.8512, available online at http://www.idealibrary.com on IDEAL®

Variable Temperature X-Ray Diffraction Study of Bismuth Magnesium Vanadate, $BiMg_2VO_6$

I. Radosavljevic and A. W. Sleight[1]

Department of Chemistry, Oregon State University, Corvallis, Oregon 97331-4003

Received July 12, 1999; in revised form September 3, 1999; accepted September 21, 1999

The space group for the structure of $BiMg_2VO_6$ at room temperature is shown to be *Pmcn*, rather than *Amma* as previously reported. However, when $BiMg_2VO_6$, is heated, its structure adopts the *Amma* space group at about 320 K. When the temperature is decreased through this transition, the $(VO_4)^{3-}$ tetrahedron tilts, destroying one of the mirror planes in space group *Amma*. In space group *Amma* the $(BiO_2)^{1-}$ chains have four equal Bi–O distances of 2.204 Å at 350 K. However, in the lower space group, there are two sets of Bi–O distances, 2.188 and 2.223 Å at 100 K. Unit cell edges in $BiMg_2VO_6$ increase with increasing temperature, giving an average linear thermal expansion of 5.2×10^{-6} K^{-1} over the 100–350 K range.

INTRODUCTION

A series of compounds with the BiA_2MO_6 formula have been discovered where M may be pentavalent V, As, or P(1). The A^{2+} cation can be Ca, Mg, Cd, Pb, or Cu. The structures for all the compounds found of this type contain $(BiO_2)^-$ chains and $(MO_4)^{3-}$ tetrahedra. Ferroelectric behavior is found in the case of $BiCa_2VO_6$. The combination of Bi^{3+} and V^{5+} in oxides leads to a bright yellow color and possible pigment applications.

The room temperature structure of $BiMg_2VO_6$ was solved from single-crystal X-ray diffraction data in 1992 (2). The compound was reported as orthorhombic with unit-cell dimensions of $a = 7.9136(6)$ Å, $b = 12.246(2)$ Å, and $c = 5.544(2)$ Å and space group *Cmcm*, but in this paper we use the *Amma* setting for this space group. We decided to re-examine this structure because of the unusually large thermal ellipsoid found for one oxygen atom in the structure. Studying this structure as a function of temperature should reveal whether this ellipsoid describes actual unusual thermal motion or whether it reflects positional disorder. There was also the possibility that the structure had not been refined in the correct space group.

[1]Corresponding author: Fax: (541)737-4407. E-mail: sleighta@chem.orst.edu.

EXPERIMENTAL

Single crystal of $BiMg_2VO_6$ were grown from a Bi_2O_3 flux in a platinum crucible. Bi_2O_3 (Atomergic Chemetals, 99.9%), MgO (Aldrich, 99 + %), and NH_4VO_3 (Johnson Mathey, 99.99%) were mixed in a 2 : 2 : 1 molar ratio. The mixture was heated at 700°C for 12 h, at 800°C for 6 h, and at 1000°C for 1 h. It was cooled to 500°C at a rate of 0.05°/h and then furnace-cooled to room temperature. Yellow needle-shaped crystals were obtained.

Preliminary structural studies were carried out with an Enraf-Nonius DIP 2000 image plate diffractometer using Mo radiation, equipped with an Oxford Cryosystems nitrogen gas cryostream. Oscillation photographs of several different crystals were taken in 3° intervals, with exposure time of 900 s. Two data sets were collected, one at room temperature and the other at 150 K. In both cases, 60 frames were recorded at 3° intervals, with an exposure time of 900 s per frame. The images obtained were processed using the XDisplayF, Denzo, and Scalepack programs of the HKL software suite (3). Details about these data collections are given in Table 1. These data revealed the presence of weak reflections that violated the centering condition, indicating that the previously assumed space group was incorrect (2).

TABLE 1
Data Collection Using a DIP 2000 Image Plate Diffractometer

Instrument	Enraf-Nonius DIP 200 image plate diffractometer	
Wavelength (λ)	0.71073	0.71073
Temperature (K)	298	150
No. of independent reflections	663	661
No. of reflections $>3\sigma I$	461	510
R_{merge} (%)	13.6	12.7
Space group	*Pmcn*	*Pmcn*

0022-4596/00 $35.00

TABLE 2
Data Collection Information

Crystal size (mm)	$0.1 \times 0.1 \times 0.3$
Crystal shape	needle
Crystal color	yellow
Crystal system	orthorhombic
Diffractometer	Enraf-Nonius CAD4
Radiation	Cu
θ range (°)	2–75
Scan mode	2θ–ω
h range	0–6
k range	0–9
l range	0–15
No. of centering reflections	25
θ minimum of centering reflections	6.68
θ maximum of centering reflections	46.15
No. of intensity standards	3 (checked every 100 reflections)
No. of orientation standards	2 (checked every 60 min)

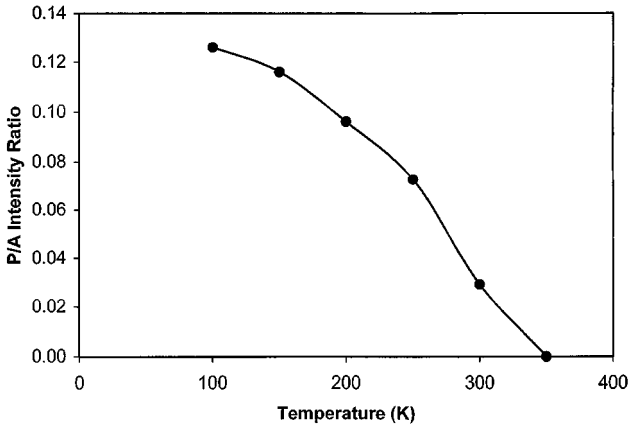

FIG. 1. Ratio of the sum of intensities for *A*- and *P*-reflections as a function of temperature.

A crystal $0.1 \times 0.1 \times 0.3$ mm^3 in dimensions was picked for complete data collection as a function of temperature. Variable temperature X-ray diffraction experiments were conducted on an Enraf-Nonius Mach3 diffractometer using Cu radiation. Data collections were performed at 100, 150, 200, 250, 300, and 350 K. Temperature was adjusted and controlled using an Oxford Cryosystems nitrogen gas cryostream. Temperatures were estimated to be accurate to within 0.1°. Twenty-five reflections were located from a combination of automated search routines and Polaroid photographs. These reflections were centered and indexed to the primitive orthorhombic cell. Data collection was then performed in the θ range from 2° to 75°. The same reflection centering file and collection conditions were used at all subsequent temperatures. Data sets were processed using RC93 software (4). Structure refinements were performed using the Oxford Crystals suite (5). Details on the crystal and general data collection conditions are given in Table 2. Temperature-dependent parameters of data collections and refinements are given in Table 3.

TABLE 3
Structure Refinement Details as a Function of Temperature

	100 K	150 K	200 K	250 K	300 K	350 K
Space group	*Pmcn*	*Pmcn*	*Pmcn*	*Pmcn*	*Pmcn*	*Amma*
Z	4	4	4	4	4	4
Density (g/cm^3)	5.136	5.134	5.130	5.126	5.120	5.116
No. of reflections	530	529	528	520	480	318
No. of parameters	56	56	56	56	56	33
Extinction	11.7(3)	11.0(3)	16.2(18)	15.6(19)	17.7(23)	3.8(8)
Scale factor	2.49(4)	2.47(4)	2.57(4)	2.52(5)	2.58(5)	1.89(4)
R (%)	5.75	6.88	6.00	6.99	6.66	8.27
wR (%)	6.68	7.46	6.62	7.43	7.76	9.47

STRUCTURAL ANALYSIS

Analysis of the diffraction images taken both at 150 K and at room temperature gave an orthorhombic cell of $a \sim 5.4$ Å, $b \sim 7.9$ Å, and $c \sim 12.2$ Å and indicated the reflection conditions of (h00): $h = 2n$; (0k0): $k = 2n$; (00l): $l = 2n$; (h0l): $l = 2n$, and (hk0): $h + k = 2n$. There were clearly no systematic absences for the (hkl) class of reflections, suggesting two possible primitive orthorhombic space groups *Pmcn* (No. 62) or $P2_1cn$ (No. 33). Because a negative second harmonic generation test for $BiMg_2VO_6$ had been reported (2), the refinements in this work were conducted in the centrosymmetric space group.

The six data sets collected between 100 and 350 K were also inspected for the presence of (hkl): $k + l = 2n + 1$ reflections. The absence of such reflections would indicate *A* centering. The intensity of the reflections requiring the primitive cell decreased with increasing temperature, and no such reflections were observed at 350 K (Fig. 1). This indicates that $BiMg_2VO_6$ undergoes a phase transition from the primitive space group *Pmcn* to its centered supergroup *Amma* somewhere between 300 and 350 K. Structure refinements at 100, 150, 200, 250, and 300 K were performed in

TABLE 4
Varation of Unit-Cell Parameters as a Function of Temperature

T (K)	a (Å)	b (Å)	c (Å)	V (Å)
100	5.4405(2)	7.9122(2)	12.2214(4)	526.09(3)
150	5.4404(2)	7.9128(2)	12.2261(4)	526.32(3)
200	5.4411(2)	7.9142(1)	12.2313(3)	526.70(3)
250	5.4420(2)	7.9152(2)	12.2384(3)	527.16(3)
300	5.4431(2)	7.9160(2)	12.2475(3)	527.72(3)
350	5.4449(4)	7.9169(5)	12.2522(7)	528.15(6)

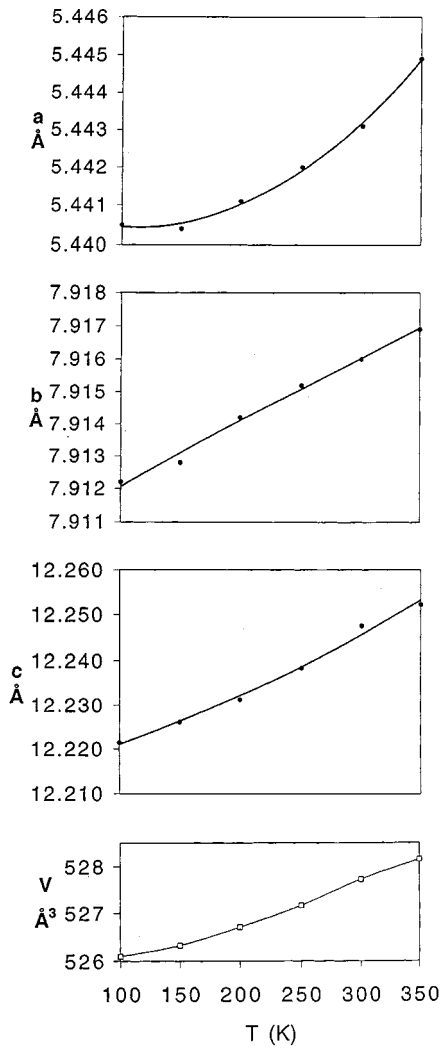

FIG. 2. Unit-cell dimensions as a function of temperature.

space group *Pmcn*. At 350 K, a free refinement in *Pmcn* was not well-behaved, but space group *Amma* gave good results.

Unit-cell parameters increased smoothly with temperature (Table 4 and Fig. 2). The increase in all four cases followed a smooth trend, suggesting that the nature of the structural change is displacive and second-order-like. This is consistent with the fact that we could find no evidence of a transition from differential scanning calorimetry.

In the primitive space group, the O1 and O2 atoms are in general positions; V, Mg2, and O3 are in $\frac{1}{4}$, y, z positions; Bi, Mg1, and O4 are in $\frac{3}{4}$, y, z positions. The refined atomic positions at different temperatures are given in Table 5. Bond lengths as a function of temperature are given in Tables 6 and in Fig. 3.

Figures 4 shows the anisotropic thermal ellipsoids of the structures obtained at different temperatures. It appears that the most striking, although not the only, difference among them is the size of the thermal ellipsoids on the O3 and O4 atoms. Table 7 summarizes the calculated isotropic equivalents of anisotropic temperature factors for all atoms. They are plotted as a function of temperature in Fig. 5. This plot shows a clear division of atoms in this structure into two classes, on the basis of the rate of change of their temperature factors. Thermal factors of O3 and O4 increase

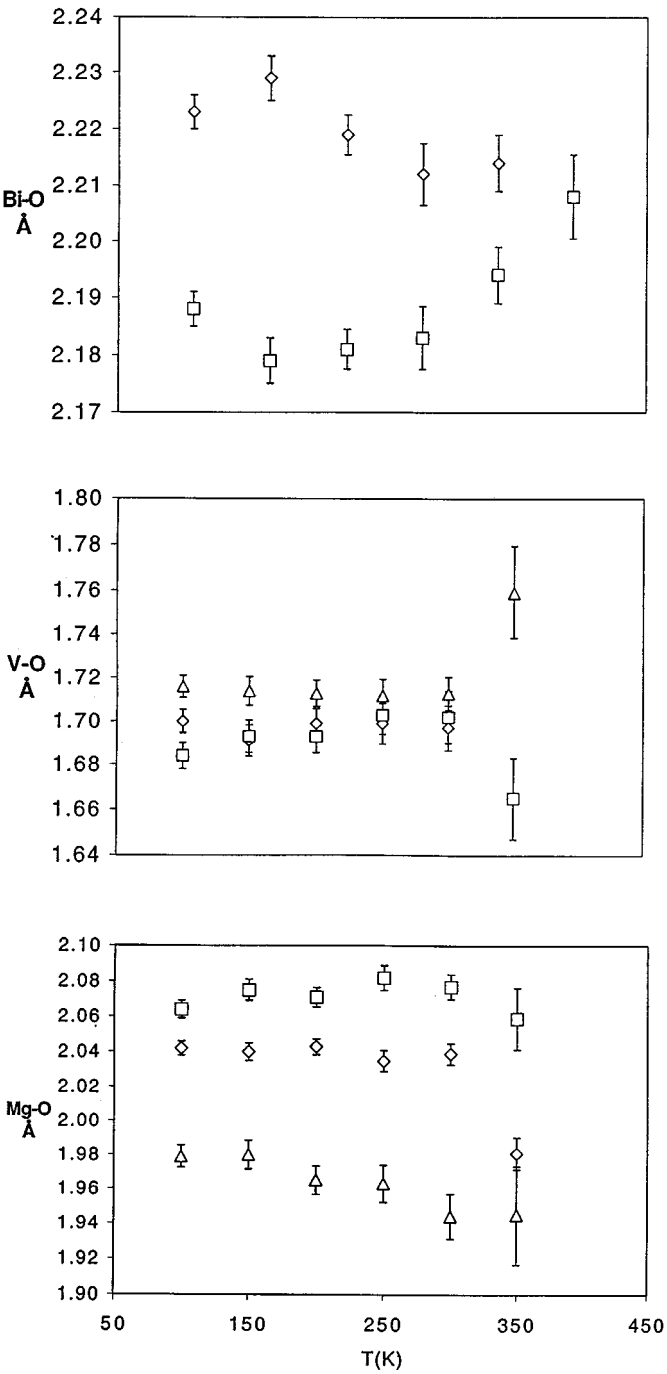

FIG. 3. Bond lengths as a function of temperature.

TABLE 5
Refined Positional Coordinates

	100 K	150 K	200 K	250 K	300 K	350 K
Bi (*x*)	0.75	0.75	0.75	0.75	0.75	0.75
Bi (*y*)	− 0.0105(1)	− 0.0099(1)	− 0.0089(1)	− 0.0076(1)	− 0.00489(9)	0.00
Bi (*z*)	0.90782(5)	0.90791(6)	0.90787(6)	0.90794(7)	0.90796(8)	0.9081(1)
V (*x*)	0.25	0.25	0.25	0.25	0.25	0.25
V (*y*)	− 0.9829(3)	− 0.9834(4)	− 0.9853(4)	− 0.9874(4)	− 0.9920(4)	− 1.00
V (*z*)	0.6981(3)	0.6983(4)	0.6979(4)	0.6974(4)	0.6973(5)	0.6965(5)
Mg1 (*x*)	0.75	0.75	0.75	0.75	0.75	0.75
Mg1 (*y*)	− 0.697(1)	− 0.696(1)	− 0.696(1)	− 0.695(1)	− 0.694(1)	− 0.691(2)
Mg1 (*z*)	0.0845(4)	0.0853(5)	0.0856	0.0863(6)	0.0875(6)	0.0885(7)
Mg2 (*x*)	0.25	0.25	0.25	0.25	0.25	0.25
Mg2 (*y*)	− 0.688(1)	− 0.689(1)	− 0.690(1)	− 0.690(1)	− 0.691(1)	− 0.691(2)
Mg2 (*z*)	0.9068(4)	0.9068(4)	0.9069(4)	0.9076(6)	0.9081(6)	0.9115(7)
O1 (*x*)	− 0.007(2)	− 0.008(3)	− 0.008(2)	− 0.008(3)	− 0.009(3)	− 0.014(5)
O1 (*y*)	− 0.9937(7)	− 0.994(1)	− 0.9948(9)	− 0.995(1)	− 0.997(1)	− 1.00
O1 (*z*)	0.6172(9)	0.618(1)	0.618(1)	0.618(1)	0.618(1)	0.617(2)
O2 (*x*)	0.001(1)	0.003(1)	0.001(1)	0.002(2)	0.001(2)	0.00
O2 (*y*)	− 0.8335(9)	− 0.834(2)	− 0.835(1)	− 0.835(1)	− 0.834(1)	− 0.834(2)
O2 (*z*)	0.9941(4)	0.9946(6)	0.9955(5)	0.9958(8)	0.9972(6)	1.00
O3 (*x*)	0.25	0.25	0.25	0.25	0.25	0.25
O3 (*y*)	− 0.140(1)	− 0.140(2)	− 0.144(2)	− 0.147(2)	− 0.56(3)	− 0.167(4)
O3 (*z*)	0.7928(9)	0.792(1)	0.791(1)	0.790(2)	0.787(2)	0.780(3)
O4 (*x*)	0.75	0.75	0.75	0.75	0.75	0.75
O4 (*y*)	− 0.292(2)	− 0.293(2)	− 0.296(2)	− 0.299(2)	− 0.307(3)	− 0.333(4)
O4 (*z*)	0.7409(9)	0.739(1)	0.737(1)	0.735(2)	0.732(2)	0.720(3)

at similar rates, about 3 times faster than the other atoms, indicating the key role of these atoms in the phase transition in question. The thermal parameters are highly correlated with coordination number, as expected. Atoms with a coordination of four or more have low thermal parameters, which are nearly all the same. The two-coordinate oxygen atoms (O3 and O4) have the highest thermal parameters. Intermediate behavior is observed for three-coordinate O1.

DISCUSSION

The temperature dependence of the intensity of superstructure reflections from 100 to 300 K (Fig. 1) suggests that the phase transition in $BiMg_2VO_6$ occurs close to 325 K. The phase transition upon heating can be described in terms of the emergence of a mirror plane perpendicular to the *y* axis, which gives rise to *A* centering in the structure. In the

TABLE 6
Bond Lengths (Å)

	100 K	150 K	200 K	250 K	300 K	350 K
Bi–O2	2.223(6) (×2)	2.229(8) (×2)	2.219(7) (×2)	2.212(11) (×2)	2.214(10) (×2)	2.204(8) (×4)
Bi–O2	2.188(6) (×2)	2.179(8) (×2)	2.181(7) (×2)	2.183(11) (×2)	2.194(10) (×2)	
V–O1	1.71(1) (×2)	1.71(1) (×2)	1.71(1) (×2)	1.71(1) (×2)	1.71(1) (×2)	1.74(2) (×2)
V–O3	1.70(1)	1.69(1)	1.70(1)	1.70(2)	1.70(2)	1.67(3) (×2)
V–O4	1.68(1)	1.69(1)	1.69(1)	1.70(2)	1.70(2)	
Mg1–O1	2.04(1) (×2)	2.04(1) (×2)	2.04(1) (×2)	2.03(1) (×2)	2.04(1) (×2)	2.02(2) (×2)
Mg1–O2	2.064(8) (×2)	2.07(1) (×2)	2.071(9) (×2)	2.08(1) (×2)	2.08(1) (×2)	2.07(1) (×2)
Mg1–O3	1.98(1)	1.98(2)	1.96(2)	1.96(2)	1.94(3)	1.97(3)
Mg2–O1	2.04(1) (×2)	2.04(1) (×2)	2.04(1) (×2)	2.03(1) (×2)	2.04(1) (×2)	2.02(2) (×2)
Mg2–O2	2.064(8) (×2)	2.071(1) (×2)	2.071(9) (×2)	2.08(1) (×2)	2.08(1) (×2)	2.07(1) (×2)
Mg2–O4	1.98(1)	1.98(2)	1.96(2)	1.96(2)	1.94(3)	1.97(3)

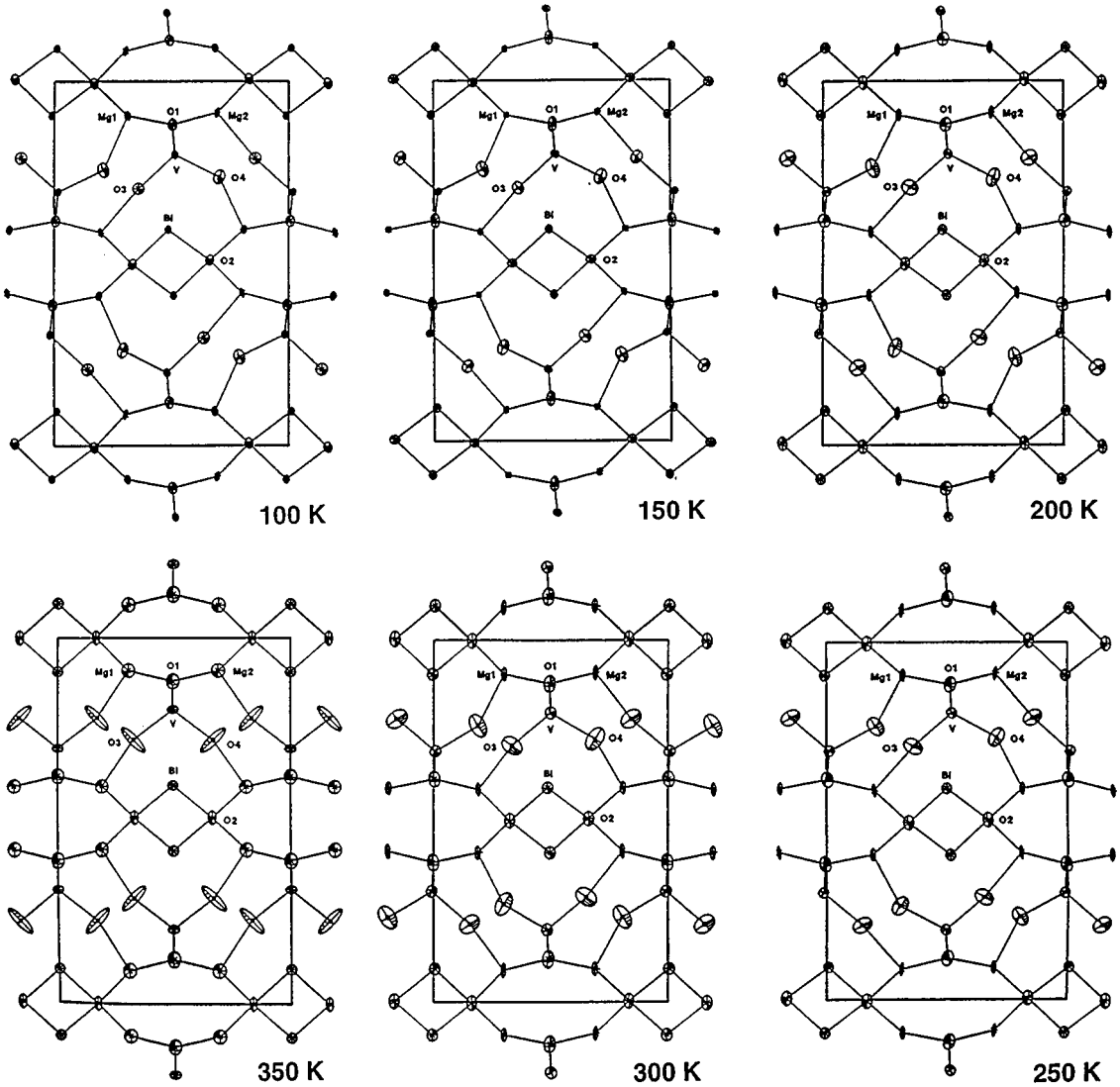

FIG. 4. Anisotropic thermal ellipsoids (50% probability) as a function of temperature.

centered structure, O3 and O4 become crystallographically equivalent, as do Mg1 and Mg2. The Bi, V, and O1 atoms move onto this mirror plane, while O2 moves onto the 2-fold axis generated by the mirror plane. These tendencies are reflected in the way that atomic coordinates change with increasing temperature. At the same time, thermal displacements of atoms increase. Table 8 summarizes the thermal displacements of atoms expressed as real principal axes of

TABLE 7
Isotropic Equivalent of Thermal Displacement Factors (Å^2) as a Function of Temperature

T (K)	Bi	V	Mg1	Mg2	O1	O2	O3	O4
100	0.0068(5)	0.0073(7)	0.009(1)	0.009(1)	0.013(2)	0.010(1)	0.013(2)	0.019(2)
150	0.0087(5)	0.0095(8)	0.011(1)	0.009(1)	0.019(2)	0.009(1)	0.017(2)	0.022(2)
200	0.0119(5)	0.0121(7)	0.014(1)	0.013(1)	0.019(2)	0.015(2)	0.023(2)	0.028(3)
250	0.0142(6)	0.0151(9)	0.015(2)	0.015(2)	0.023(2)	0.016(2)	0.028(4)	0.034(4)
300	0.0169(6)	0.0179(9)	0.017(2)	0.017(2)	0.025(2)	0.018(2)	0.038(4)	0.046(4)
350	0.012(1)	0.014(2)	0.020(3)	0.020(3)	0.024(6)	0.013(3)	0.050(8)	0.050(8)

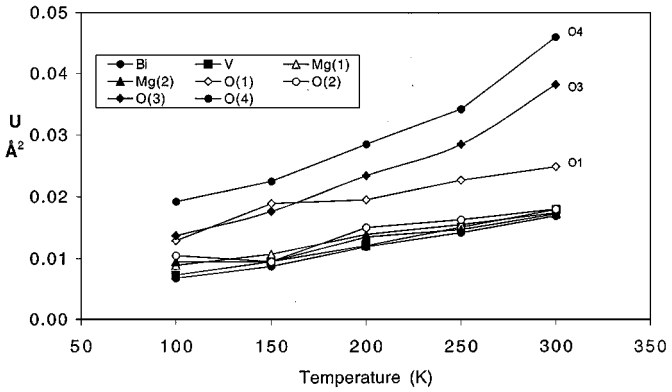

FIG. 5. Isotropic equivalents of the temperature factors as a function of temperature.

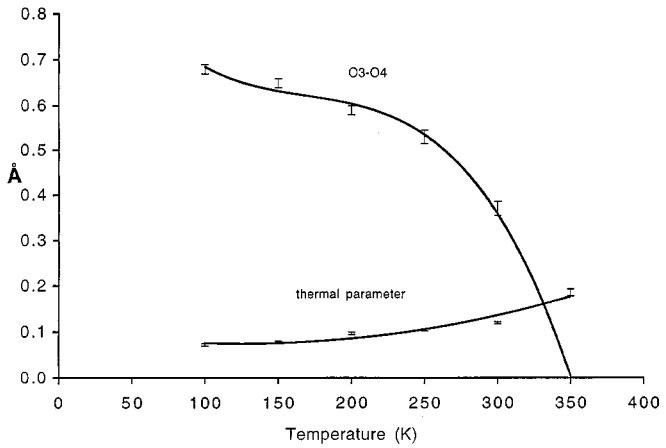

FIG. 6. Temperature dependence of the distance between the positions of O3 and O4 reflected through the mirror plane present in *Amma*, and the temperature dependence of one-half the average of the thermal displacements of O3 and O4 along their longest ellipsoid axes.

their thermal ellipsoids. The direction cosines for these axes do not change significantly as a function of temperature. This can be seen by the projections of thermal ellipsoids in Fig. 4.

The phase transition itself can be viewed as a cooperative effect of changes of atomic positions and thermal displacements. One way that this may be thought of is as follows.

TABLE 8
Principal Thermal Ellipsoid Axes (Å²) as a Function of Temperature

	100 K	150 K	200 K	250 K	300 K	350 K
Bi	0.0048	0.0066	0.0095	0.0115	0.0143	0.0101
	0.0075	0.0093	0.0128	0.0151	0.0178	0.0123
	0.0082	0.0103	0.0134	0.0159	0.0187	0.0132
V	0.0045	0.0066	0.0088	0.0113	0.0150	0.0090
	0.0078	0.0083	0.0116	0.0147	0.0172	0.0129
	0.0095	0.0137	0.0159	0.0195	0.0216	0.0209
Mg1	0.0026	0.0035	0.0025	0.0016	0.0025	0.0168
	0.0104	0.0063	0.0173	0.0194	0.0227	0.0203
	0.0139	0.0223	0.0220	0.0255	0.0270	0.0231
Mg2	0.0044	0.0036	0.0025	0.0034	0.0044	0.0168
	0.0087	0.0045	0.0159	0.0176	0.0209	0.0203
	0.0154	0.0203	0.0220	0.0232	0.0261	0.0231
O1	0.0057	0.0089	0.0109	0.0154	0.0155	0.0141
	0.0101	0.0183	0.0158	0.0158	0.0176	0.0251
	0.0231	0.0295	0.0318	0.0368	0.0418	0.0337
O2	0.0078	0.0070	0.0103	0.0094	0.0127	0.0055
	0.0105	0.0096	0.0135	0.0131	0.0141	0.0108
	0.0134	0.0119	0.0214	0.0264	0.0271	0.0236
O3	0.0079	0.0144	0.0130	0.0189	0.0273	0.0164
	0.0162	0.0175	0.0252	0.0232	0.0278	0.0305
	0.0171	0.0210	0.0320	0.0435	0.0593	0.1034
O4	0.0134	0.0145	0.0166	0.0207	0.0265	0.0164
	0.0178	0.0240	0.0255	0.0357	0.0425	0.0305
	0.0263	0.0290	0.0432	0.0461	0.0691	0.1034

The changing atomic positions of O3 and O4 can be monitored by calculating the distance between, for example, O4 and the position of O3 reflected in the mirror plane that will eventually appear in the structure. This distance decreases with temperature (Fig. 6). When this distance becomes smaller than one-half of the sum of the longest real ellipsoid semiaxes on O3 and O4, these atoms overlap when reflected through the mirror plane present in *Amma*. This overlap then could precipitate the phase transition to *Amma* where the mirror plane relating O3 and O4 is actually present. A plot of these thermal parameters indicates that this critical overlap of the mirror images of O3 and O4 should occur between 300 and 350 K.

The matter of the unusually large thermal ellipsoid found for one oxygen atom in (2) has been resolved. This was partly due to the fact that the structure had been refined in an incorrect space group. However, the thermal ellipsoid for this oxygen was found to remain relatively high, even when refining $BiMg_2VO_6$ in the correct space groups of either *Pmcn* or *Amma* (Fig. 4).

REFERENCES

1. I. Radosavljevic, J. S. O. Evans, and A. W. Sleight, *J. Solid State Chem.* **141,** 149 (1998).
2. J. Huang and A. W. Sleight, *J. Solid State Chem.* **100,** 170 (1992).
3. Z. Otwinowski and W. Minor, *in* "Methods in Enzymology" (C. W. Carter, Jr. and R. M. Sweet, Eds.), p. 276. Academic Press, New York, 1996.
4. RC93 Software, Chemical Crystallography Laboratory, University of Oxford, Oxford, 1993.
5. D. J. Watkin, J. R. Carruthers, and P. W. Betteridge, OXFORD CRYSTALS. Chemical Crystallography Laboratory, University of Oxford, Oxford, 1985.
6. D. Stewart and N. Walker, *Acta Crystallogr. Sect. A* **39,** 158 (1983).